Journal of ELECTRONIC MATERIALS, Vol. 47, No. 2, 2018
DOI: 10.1007/s11664-017-5814-0

TOPICAL COLLECTION: 59TH ELECTRONIC MATERIALS CONFERENCE 2017

Deposition of Methylammonium Lead Triiodide by Resonant Infrared Matrix-Assisted Pulsed Laser Evaporation

E. TOMAS BARRAZA,[1] WILEY A. DUNLAP-SHOHL,[2] DAVID B. MITZI,[2,3] and ADRIENNE D. STIFF-ROBERTS[1,4]

1.—Department of Electrical and Computer Engineering, Duke University, Durham, NC 27708, USA. 2.—Department of Mechanical Engineering and Materials Science, Duke University, Durham, NC 27708, USA. 3.—Department of Chemistry, Duke University, Durham, NC 27708, USA. 4.—e-mail: adrienne.stiffroberts@duke.edu

Resonant infrared matrix-assisted pulsed laser evaporation (RIR-MAPLE) was used to deposit the metal-halide perovskite (MHP) $CH_3NH_3PbI_3$ (methylammonium lead triiodide, or MAPbI), creating phase-pure films. Given the moisture sensitivity of these crystalline, multi-component organic–inorganic hybrid materials, deposition of MAPbI by RIR-MAPLE required a departure from the use of water-based emulsions as deposition targets. Different chemistries were explored to create targets that properly dissolved MAPbI components, were stable under vacuum conditions, and enabled resonant laser energy absorption. Secondary phases and solvent contamination in the resulting films were studied through Fourier transform infrared (FTIR) absorbance and x-ray diffraction (XRD) measurements, suggesting that lingering excess methylammonium iodide (MAI) and low-vapor pressure solvents can distort the microstructure, creating crystalline and amorphous non-perovskite phases. Thermal annealing of films deposited by RIR-MAPLE allowed for excess solvent to be evaporated from films without degrading the MAPbI structure. Further, it was demonstrated that RIR-MAPLE does not require excess MAI to create stoichiometric films with optoelectronic properties, crystal structure, and film morphology comparable to films created using more established spin-coating methods for processing MHPs. This work marks the first time a MAPLE-related technique was used to deposit MHPs.

Key words: RIR-MAPLE, matrix-assisted pulsed laser evaporation, metal-halide perovskites, methylammonium lead iodide

INTRODUCTION

Crystalline organic–inorganic hybrid materials represent a family of compounds whose mechanical and optoelectronic properties are disparate from that of their individual components. Compared to unordered hybrid systems, like polymer-quantum dot nanocomposites, crystalline hybrid materials conform to a preferential order at the nanoscale, deriving their properties from their extended crystal structure. One such group of materials showcasing this behavior, metal-halide perovskites (MHPs),[1] have gathered significant interest as next-generation materials to make low-cost, high-efficiency ($\sim 22.1\%$[2]) photovoltaics. These unique, multi-component, hybrid crystals give rise to high absorption coefficients,[3] large exciton diffusion lengths,[4] and benign grain boundaries,[5] making them excellent absorbers in photovoltaic devices. MHPs also possess bandgaps and optoelectronic properties that are tuned easily through simple compositional changes or doping.[6–9] Their precursor materials can be processed simply with wet chemistry techniques, taking advantage of self-assembly

(Received July 13, 2017; accepted September 13, 2017; published online September 27, 2017)
E. Tomas Barraza and Wiley A. Dunlap-Shohl have contributed equally.

to be incorporated into a variety of deposition processes and device architectures. Some of the deposition techniques commonly used to deposit MHP films include (but are not limited to): single-[10] and two-step[11] coating, slot-die coating,[12] inkjet printing,[13] and physical vapor deposition methods.[14]

Extensive research into solution processing for various device architectures has yielded record-breaking power conversion efficiencies in solar cells[15]; however, it is not clear how well these approaches can be applied to more diverse, crystalline, hybrid materials that might comprise organic and inorganic components with incompatible solubility. Generally, solution processing requires a solvent that can dissolve both organic and inorganic components; yet such a solvent may not exist for novel hybrid systems. In addition, solution processing can preclude the fabrication of more complex device heterostructures, such as graded compositions or tandem solar cells. If adjacent layers in the structure have similar solubility characteristics, the solvent used to deposit the top layer may damage or destroy layers already formed beneath. Developed in parallel to solution processing, physical vapor deposition could be advantageous for the general class of crystalline hybrid materials by eliminating concerns related to solvent interactions. Since the work of Liu et al.[16] demonstrated high-efficiency planar devices using dual-source thermal evaporation, vapor techniques have been investigated for the same device designs as those used in solution processing, reaching up to 16% power conversion efficiency.[17] Challenges facing vapor deposition of MHPs are related mostly to the evaporation of the organic component, including: difficulty in attaining thick films (while maintaining stoichiometry),[14] degradation of organics (especially in laser-based evaporation[18]), and difficulty controlling film stoichiometry by deposition rates in thermal evaporation.[19]

Emulsion-based, resonant infrared matrix-assisted pulsed laser evaporation (RIR-MAPLE) is a physical vapor deposition method uniquely positioned to address these issues. RIR-MAPLE target materials are loaded into a stainless-steel cup which rotates within a liquid nitrogen-cooled stage inside a vacuum chamber. Vacuum conditions are maintained by a turbomolecular pump. Once the target is frozen and base chamber pressure (1×10^{-4} kPa) is reached, a rastering 2.94 μm Er:YAG laser initiates film deposition. Selective absorption of the laser energy occurs in the water matrix of oil-in-water emulsions (comprising an oil phase of target materials in hydrophobic solvents) by resonance with vibrational modes of hydroxyl bonds. This absorption of laser energy evaporates the water matrix and gently transfers the target materials to the substrate, which sits on a rotating platen (Fig. 1). Liquid nitrogen temperatures (−196°C) and the base threshold pressure are maintained throughout

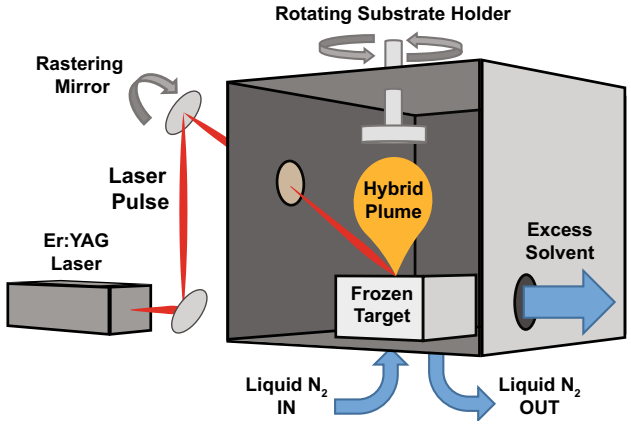

Fig. 1. Overview of simultaneous deposition of MAPbI by RIR-MAPLE. Energy from an infrared Er:YAG laser source is absorbed selectively by the solvent matrix, which is subsequently vaporized. A plume of both organic and inorganic components is created and maintained in the vacuum environment, where the individual components can travel kinetically to the chosen substrate while excess solvent is pumped away.

the length of the deposition (usually 2–4 h) to ensure that the target remains frozen and that excess solvent is pumped away by the turbomolecular pump, respectively. RIR-MAPLE has demonstrated the capability to deposit a variety of organic and inorganic materials,[20–22] and importantly, this thin-film growth mechanism eliminates the degradation of organic components that occurs in other physical vapor deposition approaches.[23] Because RIR-MAPLE deposits films in a 'dry' manner (i.e., reduces the amount of solvent which reaches the film, but does not completely eliminate the solvent from the process), the technique is applicable to any substrate choice.[20] Further, the sequential deposition mode of individual components in RIR-MAPLE has been shown to effectively deposit organic–inorganic hybrid nanocomposites (i.e., semiconductor nanoparticles in polymer matrices) with nanoscale blending of the individual components.[24,25] An important advantage of using RIR-MAPLE for crystalline organic–inorganic hybrid materials, compared to solution processing, is that its versatility enables deposition of immiscible components. Specifically regarding MHP deposition by RIR-MAPLE, this versatility could enable: i) the incorporation of novel organic cations with solubility characteristics that are incompatible with lead halide salts (which are notoriously insoluble in all but a handful of very polar solvents), and ii) the development of complex device heterostructures that are inaccessible by solution processing. In this work, the widely studied hybrid MHP, $CH_3NH_3PbI_3$ (methylammonium lead triiodide, or MAPbI), is investigated to explore the applicability of RIR-MAPLE to the deposition of MHPs, and more generally, crystalline hybrid materials. An important challenge addressed in this work is the development of new target chemistries that eliminate

water-based emulsions (due to the negative impact of water on MHPs), yet provide an appropriate matrix for resonant laser absorption.

EXPERIMENTAL METHODS

Materials

Methylammonium iodide (MAI) was purchased from Dyesol Inc., and lead(II) iodide (PbI_2, 99.999% purity) was purchased from Alfa Aesar. Anhydrous dimethyl sulfoxide (DMSO), *N*,*N*-dimethylformamide (DMF), methanol, ethanol, chlorobenzene, acetone, phenol, glycerol, and monoethylene glycol (MEG) were purchased from Sigma-Aldrich Corp. (now MilliporeSigma). Glass slides coated with fluorine-doped tin oxide (FTO) were purchased from Kintec Co. Glass slides coated with indium tin oxide (ITO) were purchased from Xintan Technology Ltd. Poly(3,4-ethylenedioxythiophene) poly(styrenesulfonate) (PEDOT:PSS; Clevios™ PVP Al 4083) was purchased from Heraeus Group. Titanium diisopropoxide bis(acetylacetonate) as a 75 wt.% solution in isopropanol ($Ti(acac)_2$) was obtained from Sigma-Aldrich. All materials were used as received without further purification.

Substrate Preparation

ITO-coated glass substrates were first submerged and sonicated for 10 min in acetone, methanol, and isopropanol, respectively. Substrates were then dried and transferred into a plasma asher to undergo a 10-min oxygen plasma cleaning. PEDOT:PSS films were created according to the procedure described in Ref. 21. FTO substrates were sequentially cleaned in Alconox detergent, deionized water, acetone, and isopropanol for 10 min each, and baked at 540°C on a hot plate for 1 h before use. TiO_2 thin films were synthesized in air by spraying a solution of two parts $Ti(acac)_2$ in one part ethanol onto FTO substrates on a hot plate set to 450°C, thereafter annealing the substrates at 500°C for 1 h. Spin-cast reference $MAPbI_3$ films were deposited onto clean glass substrates from a DMF/DMSO solution using the method described in Ref. 26.

Resonant Infrared Matrix-Assisted Pulsed Laser Evaporation Deposition Target Preparation and Post-Deposition Processing

MHP precursor materials, MAI and PbI_2, were pre-measured and dissolved in different solvents or solvent combinations to yield the desired molar/volume ratios and/or concentrations to be used as targets for RIR-MAPLE deposition. At a minimum, suitable target chemistries comprise good solvent(s) for the material(s) to be deposited [i.e., primary solvent(s)], a low-vapor pressure solvent to prevent target sublimation in vacuum, and a solvent matrix containing hydroxyl bonds for resonant laser absorption. Solvents which are selected to perform these functions individually are described as the primary, low-vapor pressure, and matrix solvents, respectively. In some cases, depending on the solvent chemistry, a single chemical can provide one or more of these functions. In the current study, two general types of target chemistries were considered.

First, in analogy to emulsion-based targets,[21] phenol was included as a low-vapor pressure solvent with primary solvent-to-low-vapor pressure solvent-to-matrix solvent compositions of 1:2:2 (by vol.%). In this triple-solvent approach, DMF (a good solvent for MAI and PbI_2) acted as the primary solvent, and the matrix solvent choice was investigated (ethanol versus methanol). It is important to note that the use of phenol as a low-vapor pressure solvent in RIR-MAPLE targets has the benefit of providing additional hydroxyl bonds to improve laser absorption. For this reason, phenol was also investigated as a matrix solvent, and chlorobenzene or acetone (which both lack hydroxyl bonds) were included as third solvent components to determine the impact of their selective solubility (i.e., chlorobenzene is a good solvent for the organic component and acetone is a good solvent for the inorganic component). A molar ratio of 1:3 PbI_2-to-MAI and a total concentration of 10 mg/ml was used for these target solutions. In the case of the ethanol matrix solvent, an additional concentration of 2 mg/ml was prepared to explore the effects of concentration on the amount of precipitate in the solution and the resulting morphology of films deposited by RIR-MAPLE.

The second type of target chemistry under investigation involved polyalcohols for the incorporated matrix solvent and low-vapor pressure solvent functions in a single chemical. For this double-solvent approach, the target compositions were primary solvent-to-polyalcohol of DMSO-to-*y* (where *y* was either glycerol or MEG; 1:1 by vol.%). The concentration of PbI_2 was 10 mg/ml for these solutions, and MAI was added to give 2:1 or 1:1 MAI-to-PbI_2 molar ratios. For each target chemistry under investigation, benchtop observations of the starting mixture were followed by RIR-MAPLE deposition only if the solution was of sufficient quality (i.e., low to no precipitation of precursor materials).

All solutions were prepared in a nitrogen-filled glovebox with O_2 and H_2O levels < 0.1 ppm. Target solutions were transferred to a stainless-steel target cup within the RIR-MAPLE deposition chamber. A nitrogen purge cycle, in which the chamber pressure was cycled from 1.33 kPa to 13.33 kPa, was performed to prevent the condensation of moisture as the target was cooled by liquid nitrogen. The cycling continued until the target temperature reached −196°C, at which point nitrogen gas was used to raise chamber pressure to $\sim$ 33–36 kPa. This pressure was held to allow the solution inside the evaporation target to freeze solid. After pumping the chamber back down past the 1×10^{-4}-kPa threshold, the RIR-MAPLE process was started. A

pulse repetition frequency of 2 Hz and laser fluence of 125–135 mJ/cm^2 were used for all depositions. The target-to-substrate distance was 7 cm. The target rotation was maintained at 4 RPM to achieve uniform evaporation of the target by a laser raster pattern. The duration of RIR-MAPLE depositions ranged from 2 h to 4 h. Some films were heated during the deposition to 75°C by an infrared lamp located above the substrates. After deposition, some films were subject to post-processing by thermal annealing at 110°C, 130°C, or 150°C for 10 min on a hotplate in a nitrogen environment.

Materials Characterization

X-ray diffraction (XRD) spectra were obtained to observe the crystallographic phase purity of deposited films (as compared to spin-cast references) using a Panalytical Empyrean x-ray diffractometer with Cu K-α radiation using operating voltage and current set at 40 kV and 40 mA, respectively. Scanning electron microscopy (SEM) images were obtained to observe the effects of different chemistries and process steps on film morphology (compared to spin-cast references where applicable). Images were obtained using an FEI XL30 SEM-FEG system with the accelerating voltage set at 5 kV. Fourier transform infrared (FTIR) absorbance spectra were obtained to explore the presence of excess solvent in films and the effects of annealing. FTIR spectra were collected using a Thermo Electron Nicolet 8700 system in attenuated total reflectance mode. Photoluminescence spectroscopy measurements were obtained using a Horiba Jobin Yvon LabRam ARAMIS system with a 633 nm HeNe laser as the excitation source, to monitor any effects of the film deposition and post-processing on the optoelectronic properties of the material compared to spin-cast references.

RESULTS AND DISCUSSION

MAPbI Target Chemistry

Three main criteria determine the required properties of MAPbI target solutions for RIR-MAPLE deposition. First, the primary solvent must provide a precipitate-free solution of MAI and PbI_2 precursors. PbI_2 is soluble only in polar solvents, which limits the options for creating a single precursor solution.[27] Second, the overall vapor pressure of the solution should be sufficiently low to prevent significant sublimation of the target due to the vacuum conditions of the growth chamber. Third, a sufficient concentration of hydroxyl bonds must be provided to enable the resonant absorption of laser energy. As shown in Table I, primary polar solvents that can dissolve both MAI and PbI_2 exist (e.g., DMF, DMSO, and γ-butyrolactone), but the lack of hydroxyl groups within the corresponding molecular structures, necessitates an additional solvent to serve as the matrix (e.g., propylene glycol, ethylene glycol, glycerol, phenol, methanol, ethanol, 1-propanol). Phenol or polyalcohols (e.g., propylene glycol, MEG, glycerol) can be added to the solution to fulfill the roles of both the matrix and low-vapor pressure solvent. Matrix solvents with high vapor pressures (e.g., methanol, ethanol, 1-propanol) typically require the addition of phenol as a low-vapor pressure solvent to prevent significant target sublimation from occurring. It is important to note that while water is not an appropriate solvent component for MHPs, it is included in Table I for comparison because it is the standard matrix solvent used in emulsion-based RIR-MAPLE.

Figure 2a shows an image of solutions prepared using the triple-solvent approach, demonstrating that ethanol, methanol, chlorobenzene, and acetone lead to solutions that appear cloudy with undissolved particles (PbI_2, MAI, phenol, a combination of these, or their solute–solvent complexes). The presence of undissolved components large enough to be visually apparent is not optimal for RIR-MAPLE deposition because larger particles are harder to transfer to the substrate, thereby compromising the ability to maintain the stoichiometry of the MAPbI solution in the deposited film. While ethanol is a reasonable candidate for a matrix solvent due to its high density of hydroxyl bonds and its similar polarity and vapor pressure to water (as shown in Table I), no solvent combination yielded the desired precipitate-free solution. Nonetheless, two target solutions comprising the ethanol solvent matrix and different MAPbI precursor concentrations were deposited onto glass substrates by RIR-MAPLE. Sparse, discontinuous coverage with visually apparent phenol contamination in the form of white dendritic crystals (see supplementary figure S1) suggested that the combination of concentration of hydroxyl groups and solution characteristics were not ideal for RIR-MAPLE deposition in this case.

Figure 2b and c shows target solutions prepared using polyalcohols (glycerol and MEG) as matrix solvents with low vapor pressures, high densities of hydroxyl bonds, and larger dipole moments (as shown in Table I) and a 1:2 molar ratio of PbI_2 to MAI. This double solvent approach demonstrated clear, precipitate-free MAPbI precursor solutions. Due to the larger dipole moments, the polyalcohols dissolved the MAPbI components and maintained miscibility with DMSO better than the solvents studied for the triple-solvent approach. Depositing MAPbI from a DMSO/glycerol solution onto unheated ITO-PEDOT/PSS substrates by RIR-MAPLE (2-h deposition time) created films that appeared to be dark and conformal to the eye (see supplementary figure S2a); however, SEM imaging revealed the morphology of these films to be discontinuous at a nanoscale, with clusters of MAPbI crystals that do not fully coalesce to form a film (see supplementary figure S2b). Extending the deposition time from 2 h to 4 h and heating the substrate during the deposition to 75°C to promote grain

Table I. Solvents explored for their compatibility with MAPbI and RIR-MAPLE processing

Solvents	Vapor pressure (kPa) @ 21°C[a]	O–H concentration (mol/cm^{-3})	Dipole moment (D)[a]
Dimethylformamide (DMF)	0.507	N/A	3.8
Dimethyl sulfoxide (DMSO)	0.093	N/A	3.96
γ-Butyrolactone (GBL)	0.06[b]	N/A	4.27[d]
Phenol	0.083	0.011	2.2
Propylene glycol	0.021	0.027	2.25[d]
Ethylene glycol	0.016	0.0357	2.31
Glycerol	2.24×10^{-5} [c]	0.041	2.56[d]
Methanol	13.732	0.024	1.7
Ethanol	6.093	0.017	1.7
1-Propanol	1.787	0.013	1.7
Water	2.533	0.055	1.87

[a]I. M. Smallwood, *Handbook of Organic Solvent Properties* (Arnold, 1996).[b]At 25°C. C. L. Yaws, Handbook of Chemical Compounds Data for Process Safety (Gulf Pub. Co, 1997).[c]At 25°C. T. E. Daubert, R. P. Danner, Taylor and Francis Group. Washington, D.C. 2001, (1998).[d]CRC Handbook of Chemistry and Physics. 96th Ed. (Taylor and Francis Group, LLC, 2016).

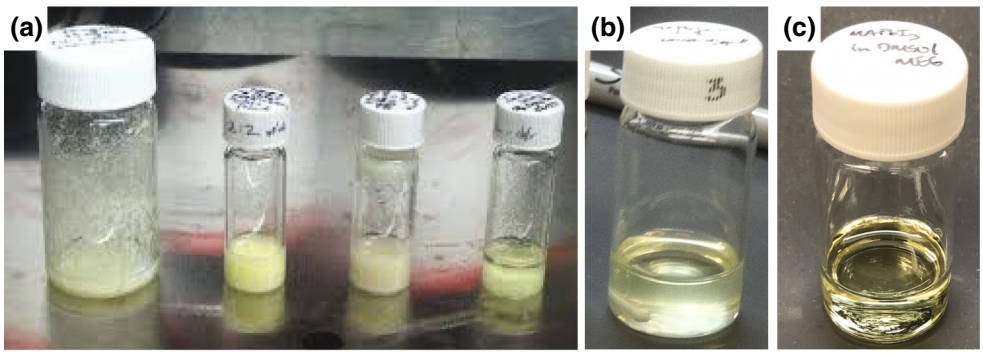

Fig. 2. PbI_2 dissolution using the multiple-solvent approach. (a) 1:2:2 DMF-to-Phenol-to-*X*, where *X* is (from left to right): ethanol, methanol, chlorobenzene, acetone. Polyalcohol as co-solvent: 1:1 DMSO-to-glycerol (b), 1:1 DMSO-to-MEG (c).

growth created dark films with coalesced small grains that eliminated most gaps and pinholes, yet contained grain boundaries that are 'blurred' instead of having a sharp contrast (Fig. 3a). This observed morphology was most likely due to contamination of the substrate by glycerol, which deposited along with the perovskite precursors during RIR-MAPLE deposition and lingered in the film due to its low vapor pressure. Depositing MAPbI from DMSO/MEG solutions by RIR-MAPLE created films that were visually similar to those using glycerol, and SEM imaging revealed possible MEG contamination on the film surface (Fig. 3b). FTIR absorbance spectra were measured from films deposited using glycerol and MEG, and compared to a reference spin-cast film (only using DMSO/DMF as solvent) to confirm the presence of polyalcohols in the MAPLE-deposited films. Figure 4 shows the spectra of three films of each type, with the O–H absorbance peak highlighted in the inset, providing a signature for the presence of polyalcohols. Both films deposited by RIR-MAPLE showed a pronounced peak in this range that was absent from the spin-cast film, leading to the suggestion that the presence of excess polyalcohol in the MAPLE films accounts for the 'blurred' grain boundaries.

Post-Deposition Annealing

Post-deposition, thermal annealing was studied as a way of improving film morphology via the evaporation of excess solvent that remains in films deposited by RIR-MAPLE from polyalcohols in the double-solvent approach. Post-deposition annealing is often used to remove excess solvent and to fully crystallize MHP films in both solution- and vapor-phase processing. The annealing recipe must use temperatures and times that evaporate solvents and promote crystal formation while minimizing thermal degradation of the MAPbI films.[28,29] Commonly used temperatures for annealing MAPbI films usually range from 70°C to 150°C, depending on the process. For the double-solvent approach in RIR-

MAPLE, both the polyalcohols which contaminate the MAPbI films possess boiling points higher than this range (~ 290°C for glycerol, ~ 198°C for MEG); however, DMSO (boiling point ~ 189°C) can be evaporated successfully using this range of 'safe' annealing temperatures.[30] Therefore, DMSO/MEG solutions were investigated for the annealing studies, due to the considerably higher vapor pressure of MEG compared to glycerol, indicating that it could be removed from the MHP films more readily.

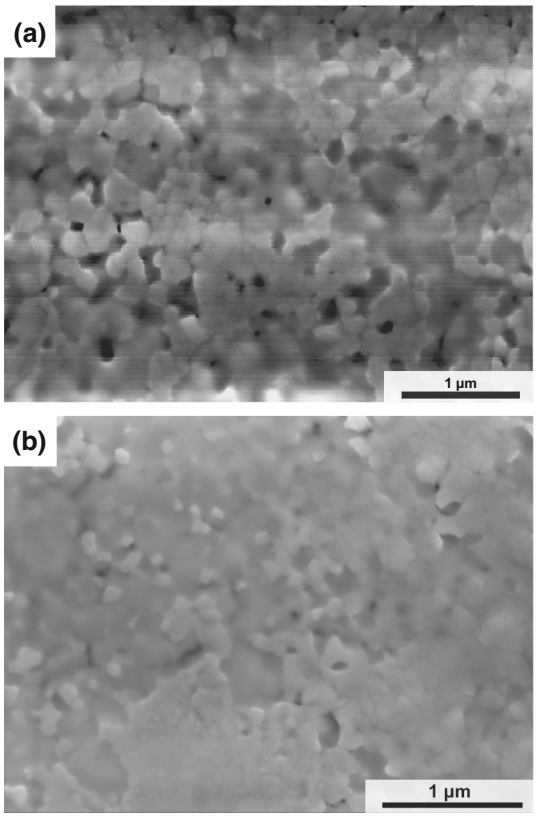

Fig. 3. SEM images of unannealed films deposited by RIR-MAPLE onto ITO/PEDOT:PSS over 4 h from (a) 1:1 DMSO-to-glycerol and (b) 1:1 DMSO-to-MEG solutions.

Figure 5 shows a comparison among FTIR absorbance spectra obtained from films that have undergone three different annealing conditions, as well as a non-annealed reference, for RIR-MAPLE deposition using the DMSO/MEG (1:1 by vol.%) double-solvent approach. A decrease in the intensity of the O–H absorption peak can be observed as the annealing temperature increases, confirming that annealing can remove excess MEG solvent matrix from the MAPbI films. XRD data (Fig. 6) also demonstrate that, while the as-deposited films contain a non-perovskite secondary phase indicated by the peaks near 11.5°, as the annealing temperature is increased, the secondary phase peak weakens and is no longer evident at 150°C, yielding phase-pure MAPbI. Similar features have been observed in XRD patterns of perovskite films grown with MAI-rich stoichiometry and assigned to an iodoplumbate precursor of undetermined chemical formula[31,32]; these or related phases may be present in the RIR-MAPLE films and principally related to the excess MAI used in the precursor target, while MEG may be present in the films in an amorphous state and thus not evident from XRD. While the XRD pattern and FTIR spectrum of the 150°C-annealed RIR-MAPLE perovskite indicate a phase-pure and polyalcohol-free film, SEM images reveal that such films deposited on ITO/PEDOT:PSS substrates contain a high density of pinholes (Fig. 7), most likely formed at least in part by the evaporation of excess solvent and MAI.

MAPbI Component Concentration

Due to known difficulties in monitoring the evaporation rate of MAI,[19] and the possible loss of MAI due to vacuum conditions (during transit to the substrate or after adsorbing to the substrate surface), as observed in other vapor processing

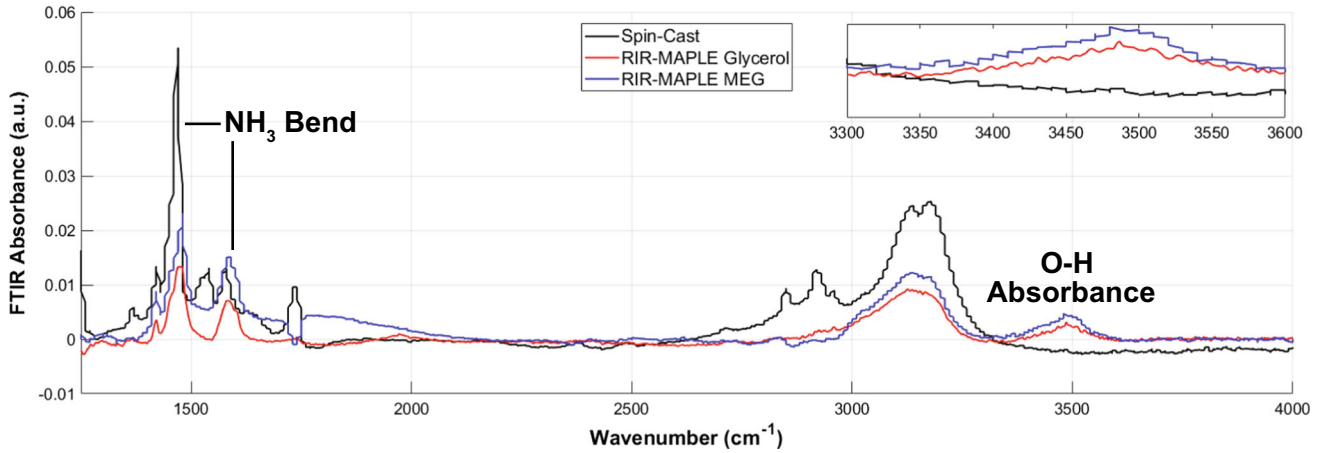

Fig. 4. FTIR spectra of films deposited by RIR-MAPLE using 1:1 DMSO-to-glycerol and 1:1 DMSO-to-MEG solutions and additional spin-cast reference. The inset shows an ~ 3500 cm^{-1} O–H absorbance peak, correlated to polyalcohol contamination of films.

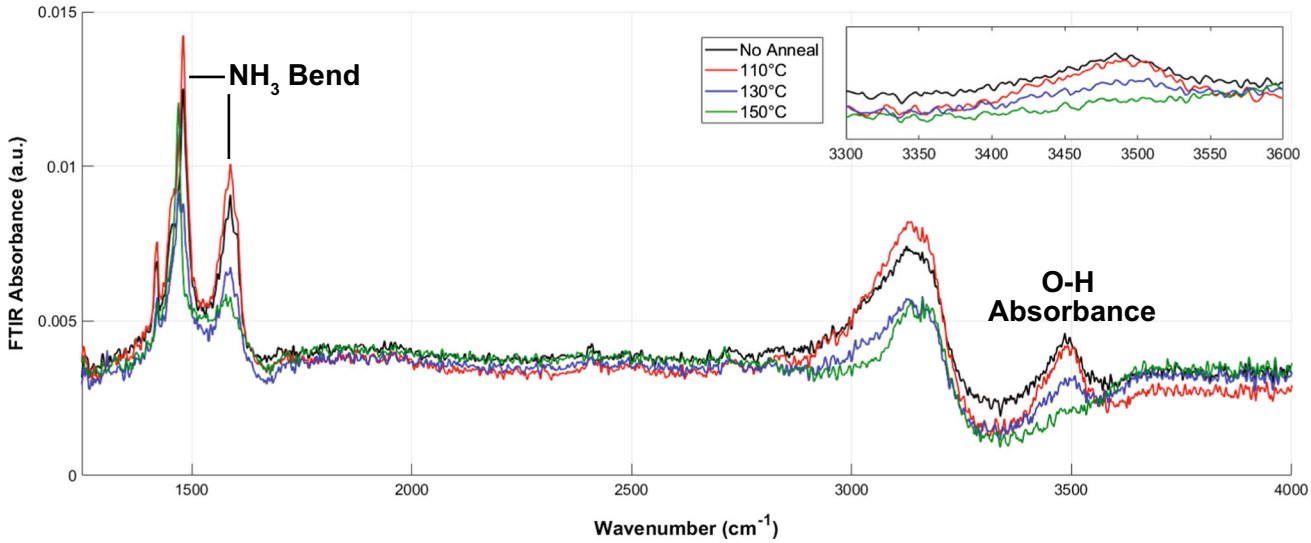

Fig. 5. FTIR spectra of films deposited by RIR-MAPLE using 1:1 DMSO-to-MEG solutions and then subjected to 10-min thermal annealings of varying temperature. The inset shows an ~ 3500 cm^{-1} O–H absorbance peak, correlated to polyalcohol contamination of films.

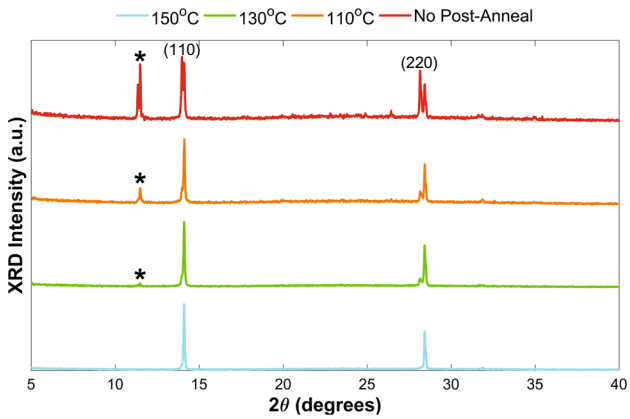

Fig. 6. X-ray diffraction spectra of films deposited by RIR-MAPLE and subjected to 10-min thermal annealings. Potential iodoplumbate complexes are indicated by (*). The MAPbI (110) peak and its reflections are marked.

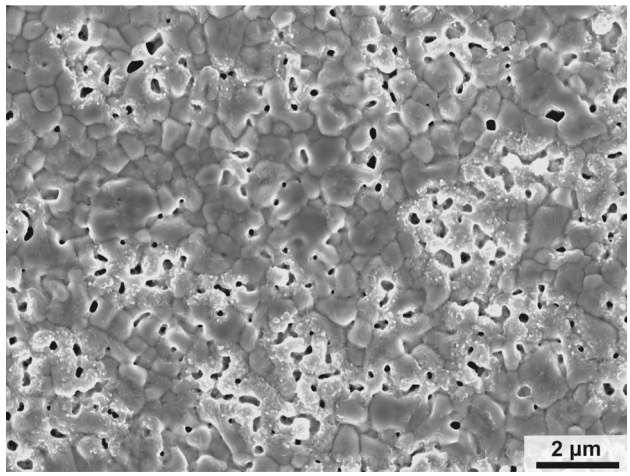

Fig. 7. SEM image of film deposited by RIR-MAPLE using a 1:1 DMSO-to-MEG (10 mg/ml) solution onto an ITO/PEDOT:PSS substrate and then annealed at 150°C for 10 min.

approaches, a 1:2 PbI_2-to-MAI molar ratio with excess organic material was used for the initial RIR-MAPLE depositions described above. To study the effects of the target stoichiometry on the films, perovskite films at 1:2 and 1:1 PbI_2-to-MAI molar ratios were grown. In order to prevent volatile MAI from escaping the film, the substrate was unheated during the deposition. However, the 1:2 PbI_2-to-MAI molar ratio (excess MAI) yielded films with pinholes and secondary organic phases accumulating on the surface of films deposited onto glass and TiO_2, even while performing a more conservative 10-min, 110°C annealing (Fig. 8a and b, respectively). These results indicate that RIR-MAPLE can preserve organic components during deposition, and therefore, the excess MAI required for other vapor processing approaches may not be necessary. When a 1:1 PbI_2-to-MAI molar ratio was used for the DMSO/MEG double-solvent solution to prevent excess-MAI conditions during deposition, post-annealing of the films at 110°C for 10 min yielded smooth, conformal, pinhole-free films with compact grain structures (Fig. 8c and d). As shown in Fig. 9a and b, photoluminescence and XRD measurements confirm that these RIR-MAPLE-deposited MAPbI films possess comparable optoelectronic and

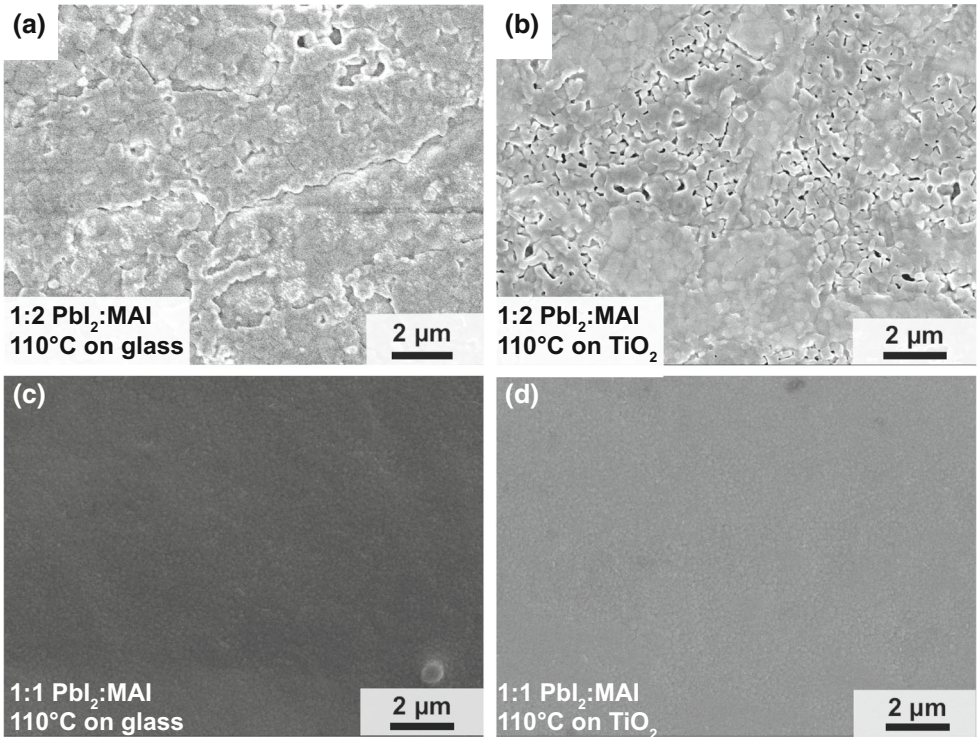

Fig. 8. SEM images of 1:2 PbI_2-to-MAI films deposited onto (a) glass, and (b) TiO_2 after a 10-min, 110°C annealing. SEM images of films with 1:1 PbI_2-to-MAI ratio deposited onto (c) glass, and (d) TiO_2 after a 10-min, 110°C annealing.

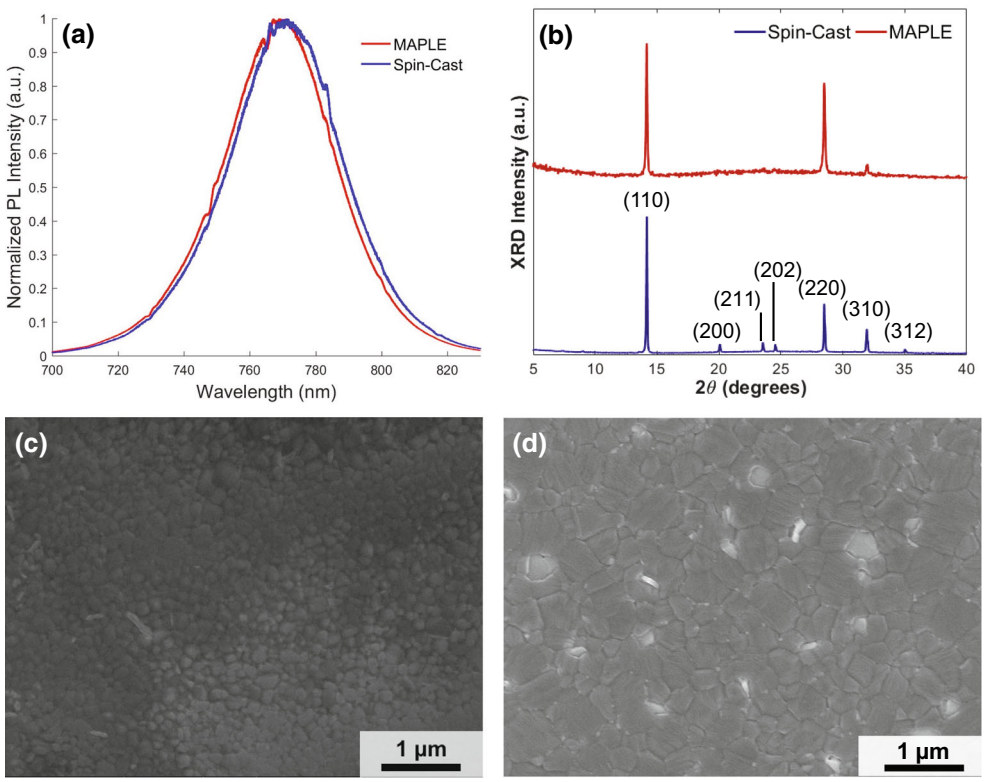

Fig. 9. (a) Photoluminescence spectrum of RIR-MAPLE-deposited film compared to a spin-cast reference. (b) X-ray diffraction spectra of films deposited by RIR-MAPLE and spin-casting, with characteristic perovskite peaks highlighted. SEM images of MAPbI film deposited by RIR-MAPLE onto TiO_2 (c), and spin-cast reference deposited onto glass (d).

crystallographic properties relative to perovskite films prepared by state-of-the-art spin-coating methods, and are thus well-suited for integration into optoelectronic devices.

CONCLUSION

In summary, this work demonstrates RIR-MAPLE deposition of MAPbI films for the first time. Smooth, pinhole-free, and phase-pure films were deposited on multiple substrates, demonstrating the versatility of this approach. The most critical aspect of selecting an appropriate target matrix for the general class of MHPs is to identify a solvent or solvent mixture that balances the dissolution of all components and possesses hydroxyl groups to enable the resonant absorption of laser energy. In general, a double-solvent mixture comprising equal parts of a polar solvent and a polyalcohol provides the required target matrix functions. Gentle thermal annealing ($\sim 110°C$ for 10 min) counteracts solvent contamination effects that result from the use of low-vapor pressure polyalcohols, which are required in the target matrix to prevent sublimation due to the vacuum conditions. Contrary to other deposition techniques, the gentle transfer of precursor materials to the substrate by RIR-MAPLE allows for stoichiometric films to be created without the use of an excess of the organic component (in this case, an MAI-to-PbI_2 ratio of 1:1). Photoluminescence and x-ray measurements show that optoelectronic and crystallographic properties, respectively, of RIR-MAPLE-deposited MAPbI films are comparable to those of perovskite films prepared by conventional spin-casting fabrication. In addition, the film morphology observed from SEM images demonstrates compact grains with well-defined grain boundaries like those of spin-cast reference films. The judicious choice of solvent matrix (i.e., MEG using the double-solvent approach) eliminates the need for water during the deposition and enables the deposition of phase-pure MAPbI by adapting emulsion-based RIR-MAPLE. The study also shows that RIR-MAPLE preserves the integrity of the organic component MAI despite the use of laser energy. This work demonstrates an important new growth paradigm for RIR-MAPLE, as well as a versatile approach for the deposition of crystalline hybrid films.

ACKNOWLEDGEMENTS

This work was supported by the National Science Foundation, Research Triangle MRSEC (DMR-1121107). We would like to acknowledge the contributions of Wangyao Ge, Yuankai Liu, and Chenqi Zhao from the Stiff-Roberts group at Duke University in developing the RIR-MAPLE methods described within this work.

CONFLICT OF INTEREST

The authors declare that they have no conflicts of interest.

ELECTRONIC SUPPLEMENTARY MATERIAL

The online version of this article (doi: 10.1007/s11664-017-5814-0) contains supplementary material, which is available to authorized users.

REFERENCES

1. D.B. Mitzi, *Progress in Inorganic Chemistry* (Hoboken: Wiley, 1999), pp. 1–121.
2. National Renewable Energy Laboratory. Best Research-Cell Efficiencies. http://www.nrel.gov/ncpv/images/efficiency_chart.jpg. Accessed 25 June 2017.
3. M.A. Green, A. Ho-Baillie, and H.J. Snaith, *Nat. Photonics* 8, 506 (2014).
4. S.D. Stranks, G.E. Eperon, G. Grancini, C. Menelaou, M.J.P. Alcocer, T. Leijtens, L.M. Herz, A. Petrozza, and H.J. Snaith, *Science* 342, 341 (2013).
5. W.J. Yin, T. Shi, and Y. Yan, *Adv. Mater.* 26, 4653 (2014).
6. G.E. Eperon, S.D. Stranks, C. Menelaou, M.B. Johnston, L.M. Herz, and H.J. Snaith, *Energy Environ. Sci.* 7, 982 (2014).
7. A.K. Guria, S.K. Dutta, S. Das Adhikari, and N. Pradhan, *ACS Energy Lett.* 2, 1014 (2017).
8. W.A. Dunlap-Shohl, R. Younts, B. Gautam, K. Gundogdu, and D.B. Mitzi, *J. Phys. Chem. C* 120, 16437 (2016).
9. S. Shahbazi, C.M. Tsai, S. Narra, C.Y. Wang, H.S. Shiu, S. Afshar, N. Taghavinia, and E.W.G. Diau, *J. Phys. Chem. C* 121, 3673 (2017).
10. W. Nie, H. Tsai, R. Asadpour, J.-C. Blancon, A.J. Neukirch, G. Gupta, J.J. Crochet, M. Chhowalla, S. Tretiak, M.A. Alam, H.-L. Wang, and A.D. Mohite, *Science* 347, 522 (2015).
11. K. Liang, D.B. Mitzi, and M.T. Prikas, *Chem. Mater.* 10, 403 (1998).
12. K. Hwang, Y.S. Jung, Y.J. Heo, F.H. Scholes, S.E. Watkins, J. Subbiah, D.J. Jones, D.Y. Kim, and D. Vak, *Adv. Mater.* 27, 1241 (2015).
13. S.-G. Li, K.-J. Jiang, M.-J. Su, X.-P. Cui, J.-H. Huang, Q.-Q. Zhang, X.-Q. Zhou, L.-M. Yang, and Y.-L. Song, *J. Mater. Chem. A* 3, 9092 (2015).
14. L.K. Ono, M.R. Leyden, S. Wang, and Y. Qi, *J. Mater. Chem. A* 4, 6693 (2016).
15. W.S. Yang, B. Park, E.H. Jung, N.J. Jeon, Y.C. Kim, D.U. Lee, S.S. Shin, J. Seo, E.K. Kim, J.H. Noh, and S. Il Seok, *Science* 356, 1376 (2017).
16. M. Liu, M.B. Johnston, and H.J. Snaith, *Nature* 501, 395 (2013).
17. D. Yang, Z. Yang, W. Qin, Y. Zhang, S.F. Liu, and C. Li, *J. Mater. Chem. A* 3, 9401 (2015).
18. D.B. Mitzi, M.T. Prikas, and K. Chondroudis, *Chem. Mater.* 11, 542 (1999).
19. S. Wang, L.K. Ono, M.R. Leyden, Y. Kato, S.R. Raga, M.V. Lee, and Y. Qi, *J. Mater. Chem. A* 3, 14631 (2015).
20. W. Ge, T.B. Hoang, M.H. Mikkelsen, and A.D. Stiff-Roberts, *Appl. Phys. A Mater. Sci. Process.* 122, 824 (2016).
21. W. Ge, N.K. Li, R.D. McCormick, E. Lichtenberg, Y.G. Yingling, A.D. Stiff-Roberts, and A.C.S. Appl, *Mater. Interfaces* 8, 19494 (2016).
22. Q. Yu, W. Ge, A. Atewologun, G.P. López, and A.D. Stiff-Roberts, *J. Mater. Chem. B* 2, 4371 (2014).

23. R.D. McCormick, J. Lenhardt, and A.D. Stiff-Roberts, *Polymers (Basel)* 4, 341 (2012).
24. W. Ge, A. Atewologun, and A.D. Stiff-Roberts, *Org. Electron.* 22, 98 (2015).
25. R. Pate, K.R. Lantz, and A.D. Stiff-Roberts, *Thin Solid Films* 517, 6798 (2009).
26. N. Ahn, D.Y. Son, I.H. Jang, S.M. Kang, M. Choi, and N.G. Park, *J. Am. Chem. Soc.* 137, 8696 (2015).
27. Y. Guo, K. Shoyama, W. Sato, Y. Matsuo, K. Inoue, K. Harano, C. Liu, H. Tanaka, and E. Nakamura, *J. Am. Chem. Soc.* 137, 15907 (2015).
28. L.C. Chen, J.R. Wu, Z.L. Tseng, C.C. Chen, S.H. Chang, J.K. Huang, K.L. Lee, and H.M. Cheng, *Materials (Basel).* 9, 747 (2016).
29. L.-C. Chen, C.-C. Chen, J.-C. Chen, and C.-G. Wu, *Sol. Energy* 122, 1047 (2015).
30. N.J. Jeon, J.H. Noh, Y.C. Kim, W.S. Yang, S. Ryu, and S. Il Seok, *Nat. Mater.* 13, 897 (2014).
31. J.S. Manser, B. Reid, and P.V. Kamat, *J. Phys. Chem. C* 119, 17065 (2015).
32. P.P. Khlyabich and Y. Loo, *Chem. Mater.* 28, 9041 (2016).